JOC The Journal of Organic Chemistry

ARTICLE

pubs.acs.org/joc

Computational Study on the Reaction Pathway of α-Bromoacetophenones with Hydroxide Ion: Possible Path Bifurcation in the Addition/Substitution Mechanism

Shuhei Itoh,[†,*] Nobuyoshi Yoshimura, Makoto Sato, and Hiroshi Yamataka*

Department of Chemistry and the Research Center for Smart Molecules, Rikkyo University, Nishi-Ikebukuro, Toshima-ku, Tokyo 171-8501, Japan

Supporting Information

ABSTRACT: The reaction of an α-haloketone with a nucleophile has three reaction channels: carbonyl addition, direct substitution, and proton abstraction. DFT calculations for the reaction of $PhCOCH_2Br$ with OH^- showed that there exists an addition/substitution TS on the potential energy surface, in which OH^- interacts with both the α- and carbonyl carbons. The intrinsic reaction coordinate calculations revealed that the TS serves as the TS for direct substitution for $XC_6H_4COCH_2Br$ with an electron-donating X or a X less electron-withdrawing than *m*-Cl, whereas the TS serves as the TS for carbonyl addition for derivatives with a X more electron-withdrawing than *m*-CF_3. Trajectory calculations starting at respective TS indicated that the single TS can serve for the two mechanisms, substitution and addition, through path bifurcation after the TS for borderline substrates. The reaction is the first example of dynamic path bifurcation for fundamental reaction types of carbonyl addition and substitution.

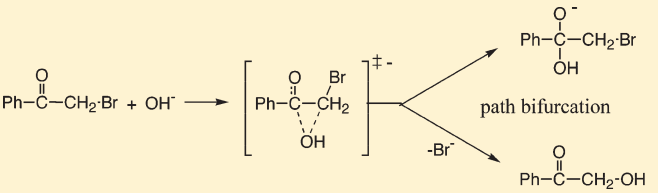

INTRODUCTION

Substitution reactions of α-haloketones have attracted much attention due to their enhanced reactivity compared to simple haloalkanes,[1] and several mechanistic schemes have been proposed to rationalize these enhanced reactivities.[2−7] It is known that α-haloketones may react at either one of the two electrophilic positions, the α-carbon (C_α) and the carbonyl carbon, depending on the nature of the nucleophile.[2,4−16] However, it is not always easy to determine the position of the initial attack on the basis of product analyses, since as can be seen in Scheme 1, the initial carbonyl-attack product may give the same final product as that from the C_α attack. At the same time, the selection between the C_α attack and the carbonyl attack may readily vary, since the HOMO of a nucleophile can interact with both the C-halogen σ* and C=O π* orbitals of an α-haloketone in a transition state (TS), as we will see later in Figure 1.

There has been growing recognition that dynamics effects affect the reaction pathways.[17] It has been shown that in some mechanistic borderline reactions, post-TS dynamics does not always follow the minimum energy path on the potential energy surface (PES) and the reaction path bifurcates on the way from the TS to product regions, giving two products from a single TS.[18] It would be important to examine the possibility that the reaction of an α-haloketone with a nucleophile gives two initial products via path bifurcation after a single TS.

The present study carried out extensive computations for the reactions of $XC_6H_4COCH_2Br$ with OH^-, which revealed that the reaction mechanism varied depending on the nature of the substrates and showed that a single TS gave two initial products (substitution and addition) for borderline cases.

Scheme 1

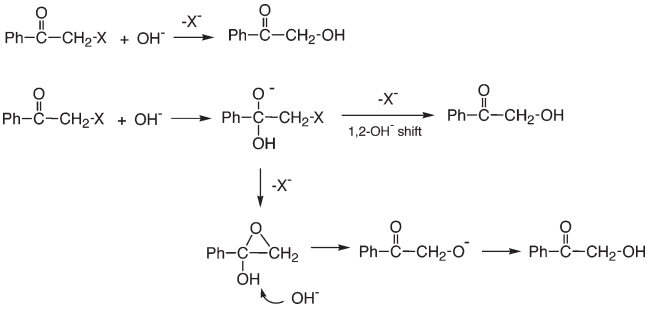

RESULTS AND DISCUSSION

Reaction Pathways and Energies. In order to examine the factors that control the reaction selectivity, addition versus substitution, DFT calculations were carried out for the reactions of $XC_6H_4COCH_2Br$ (**1**-X; X = *p*-NMe_2, *p*-NH_2, *p*-Me, *m*-Me, H, *p*-F, *p*-Cl, *m*-Cl, *m*-CF_3, *p*-CF_3, *m*-CN, *p*-CN, *m*-NO_2, *p*-NO_2) and OH^-. The structures of **1**-X, hydroxide ion, water, bromide ion, **cmp**-X, **2**-X, **3**-X, **4**-X, **TSnu**-X, **TSre**-X, and **TSab**-X were optimized at B3LYP/6-31+G*. The calculated reaction pathways for the reaction of **1**-H and OH^- are shown in Figure 1, in which relative enthalpies are given in parentheses in kcal/mol. **Cmp** is an encounter complex, and **TSnu**, **TSre**, and **TSab** are TSs of

Received: July 18, 2011
Published: September 07, 2011

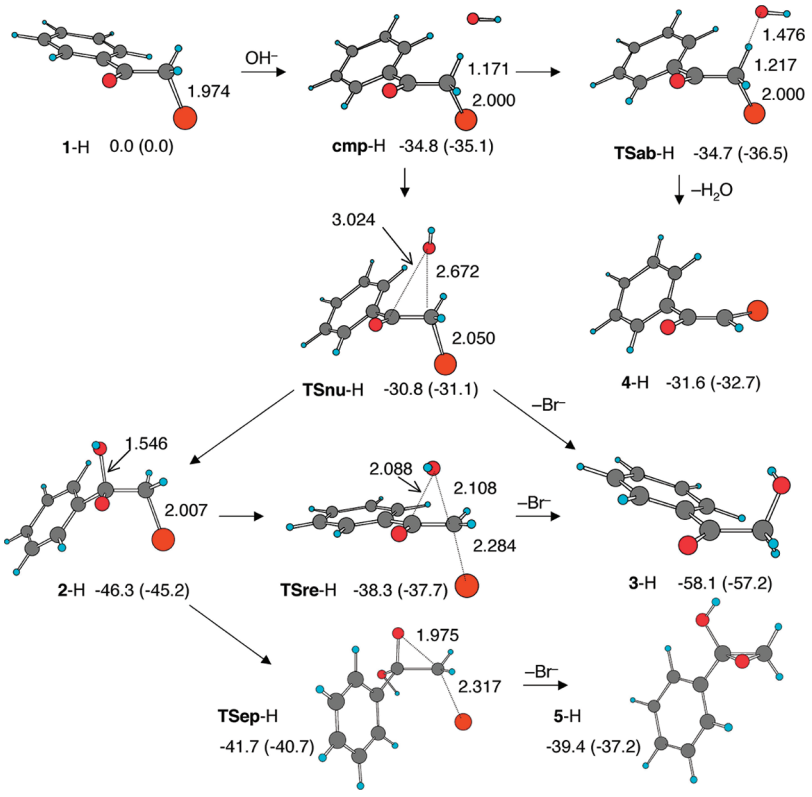

Figure 1. Reaction pathways for $PhCOCH_2Br$ and hydroxide ion at B3LYP/6-31+G*. Distances are in Å, and energies are electronic energies (enthalpies in parentheses) in kcal/mol relative to separated reactants. Energies of **1**-H, **3**-H, **4**-H, and **5**-H are those including the separated counterpart, OH^-, Br^-, H_2O, and Br^-, respectively.

nucleophilic attack, rearrangement from addition (**2**) to substitution (**3**) product, and of proton abstraction, respectively.

In **cmp**, OH^- interacts with C_α-H and *o*-H of the phenyl ring. The complex may proceed to **TSab** or **TSnu**. **TSab** has a very small barrier in electronic energy and gives the enolate anion (**4**-H), which is less stable than **cmp**. **4**-H is even less stable than **TSab**, but this is due to the lack of interaction energy between **4**-H and H_2O in the separated state. Thus, the proton abstraction is an uphill reversible step. In **TSnu**, OH^- is located on the C═O π-orbital at the carbonyl carbon and on the backside of the C−Br bond, and thus **TSnu** may give either **2** or **3**. Indeed, intrinsic reaction coordinate (IRC) calculations revealed that **TSnu** leads to **2** or **3** depending on the substituent (vide infra). The rearrangement TS (**TSre**) from **2** to **3** has a structure that is topologically similar to that of **TSnu** with much shorter $HO^-\cdots C{=}O$ (R_{O-CO}) and $HO^-\cdots C_\alpha$ ($R_{O-C\alpha}$) distances. **TSre** is lower in energy than **TSnu**, and thus if **2** is initially formed, it would give **3** as the final product rather than going back to the starting materials. Alternatively, **2** may give the epoxide intermediate, **5**, through **TSep**. The epoxide formation step has a lower activation barrier, but the epoxide intermediate is much less stable than the product alcohol. **5**-H is even less stable than **TSep**-H in the separated state. We did not examine the epoxide formation pathway in detail, since we focused on the selection in the initial addition versus substitution steps.

The C_α−Br bond length (2.050 Å) in **TSnu**-H is similar to that in **cmp** (2.000 Å). In a previous study for the reaction of α-bromoacetophenone with pyridine, the N−C and C−Br lengths at the S_N2 TS were 2.1 and 2.4 Å, respectively, at B3LYP/6-31G.[16] **TSnu**-H in the present reaction is very early, probably because of the much higher nucleophilicity of OH^-. An important point here is that **TSnu** is the only TS for the nucleophilic attack, and it is not clear from its structure whether it is the TS for substitution or for carbonyl addition.

Selected bond lengths of **TSnu**-X listed in Table 1 indicate that the structures are basically the same for all substituted derivatives. Calculated relative energies in Table 2 show that the relative energies become monotonically smaller when the substituent becomes electron-withdrawing. Linear energy plots of the relative activation enthalpies against the experimental gas-phase acidities of $XC_6H_4CO_2H$[19] are illustrated in Figure 2, which correspond to the Hammett plots in the gas phase. Here, we used enthalpies, because the size of the entropy and hence the free energy depend much on low frequencies, which are less reliable than higher frequencies, especially for compounds with weak interactions such a TS. The use of free energy gave similar correlations with more scattered points. The observed excellent correlation for all derivatives appears to suggest that the nature of the TS and the reaction mechanism do not change with substituent.

PES for the Reaction of $XC_6H_4COCH_2Br + OH^-$. The PES on the two-dimensional diagram of R_{O-CO} and the $R_{O-C\alpha}$ is shown in Figure 3. The energies are relative to the separated reactants in kcal/mol. Here, the reactant region is located in the upper-right direction. The region of large R_{O-CO} was difficult to optimize due to the presence of **TSab**-H and a complex of **4**-H and H_2O, and PES could only be constructed for the region of **TSnu**-H, **2**-H, and **3**-H. Nevertheless, it can clearly be seen that **TSnu** leads to either **2** or **3** depending on the shape of the surface.

IRC Calculations for the Reaction of $XC_6H_4COCH_2Br + OH^-$. The reaction route was analyzed by IRC calculations (Figure 4).

dx.doi.org/10.1021/jo201485y |*J. Org. Chem.* 2011, 76, 8294–8299

Table 1. Selected Bond Lengths of TSnu-X and IRC Results at B3LYP/6-31+G*[a]

X	R_{O-CO}	$R_{C\alpha-Br}$	$R_{C\alpha-Br}$	IRC
p-NMe_2	3.016	2.662	2.060	substitution
p-NH_2	3.014	2.666	2.059	substitution
p-Me	3.015	2.670	2.053	substitution
m-Me	3.032	2.674	2.051	substitution
H	3.024	2.672	2.050	substitution
p-F	3.013	2.673	2.046	substitution
p-Cl	2.998	2.672	2.043	substitution
m-Cl	2.981	2.671	2.041	substitution
m-CF_3	2.930	2.668	2.035	addition
p-CF_3	2.969	2.673	2.038	addition
m-CN	2.933	2.673	2.033	addition
p-CN	2.942	2.671	2.033	addition
m-NO_2	2.916	2.680	2.028	addition
p-NO_2	2.932	2.679	2.028	addition

[a] Bond lengths are in Å.

Table 2. Enthalpy Changes for the Reaction of $XC_6H_4COCH_2Br + OH^-$[a]

X	cmp	TSnu	2	TSre	3	TSab	4
p-NMe_2	−30.6	−26.3	−39.8	−32.2	−56.6	−31.4	−26.8
p-NH_2	−31.7	−27.5	−39.9	−33.3	−56.9	−33.4	−27.6
p-Me	−34.3	−30.1	−43.8	−36.4	−57.0	−35.7	−31.5
m-Me	−34.5	−30.3	−44.5	−36.9	−56.9	−35.8	−32.0
H	−35.1	−31.1	−45.2	−37.7	−57.2	−36.5	−32.7
p-F	−38.1	−34.2	−48.3	−40.2	−57.4	−39.6	−35.6
p-Cl	−39.1	−35.1	−49.8	−41.2	−57.4	−40.5	−37.2
m-Cl	−39.4	−35.2	−50.5	−41.8	−57.4	−40.5	−37.8
m-CF_3	−42.2	−38.1	−53.2	−44.3	−57.6	−43.3	−40.8
p-CF_3	*b*	−38.0	−53.9	−44.5	−57.4	*b*	−41.4
m-CN	−44.3	−40.2	−55.7	−46.3	−57.6	−45.4	−42.9
p-CN	*b*	−40.2	−56.5	−46.7	−57.6	*b*	−44.1
m-NO_2	−45.5	−41.9	−57.0	−47.3	−57.7	−46.8	−46.8
p-NO_2	*b*	−41.8	−58.9	−48.5	−57.7	*b*	−47.0

[a] Energies are in kcal/mol relative to the separated reactants. [b] Not determined.

It is seen that although the TS is similar and the initial directions of IRC point to the **TSre**-X region for all derivatives, IRC leads to one of the two products depending on the substituent. As shown in Figure 4 and Table 1, IRCs of substrates with a substituent more electron-withdrawing than *m*-CF_3 led to the addition product region, whereas those with a substituent less electron-withdrawing than *m*-Cl or with an electron-donating substituent reached the substitution product region. It is important to point out here that the rate-determining TS for the addition/substitution route does not have information on the product to which the TS leads and that the Hammett-type plots failed to detect the change in mechanism with substituent. This situation is similar to the Beckmann rearrangement/fragmentation,[20] the Schmidt rearrangement/fragmentation[21] and E2/E1cb borderline reactions.[22]

MD Trajectory Calculations. The DFT calculations suggested that **1**-X reacts with OH^- through a borderline mechanism, in which the mechanism changes from substitution to addition when the substituent becomes more electron-withdrawing. In such reactions a possibility exists that a single TS takes charge of two mechanisms through path bifurcation after the TS, as has been reported for other types of reactions.[18,20−23] Therefore, we have carried out direct MD simulations for the addition/substitution borderline reaction of $XC_6H_4COCH_2Br$ with OH^- to examine the possible bifurcation. Trajectory calculations on selected substrates were initiated at **TSnu**-X of each substrate at B3LYP/6-31+G* with G03[24] and PEACH v. 7.9 and 8.0.[25] Initial kinetic energy was 2.8 kcal/mol with (G03) or without (PEACH) zero-point energies on internal vibrational modes. Figure 5 shows productive trajectories for *p*-NMe_2-, *p*-Cl-, and *p*-NO_2-substituted compounds calculated with PEACH. These trajectories were classified as substitution when a trajectory reached

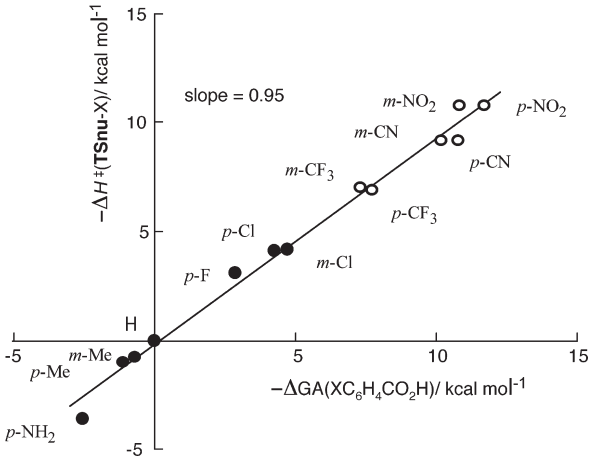

Figure 2. Hammett-type plot of relative activation enthalpies against gas-phase acidities of $XC_6H_4CO_2H$ at B3LYP/6-31+G*. Open circles are for substrates, whose IRCs led to the addition products, and closed circles are for substrates, whose IRCs gave the substitution products.

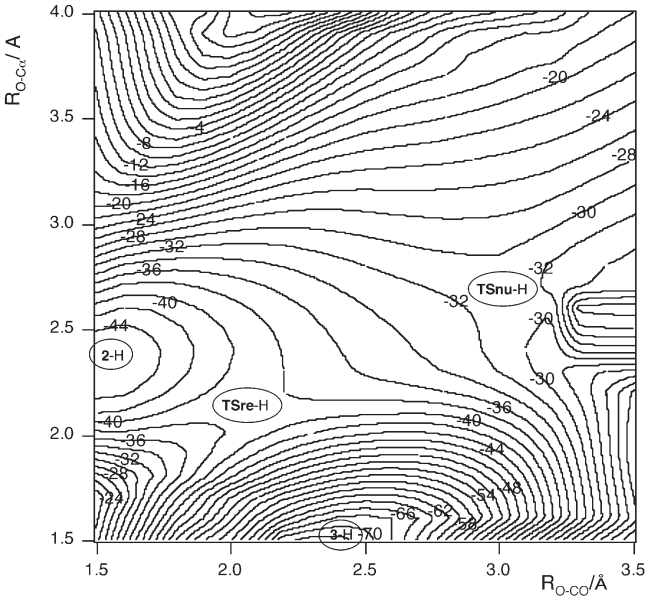

Figure 3. Two dimensional PES for the reaction of **1**H with hydroxide ion at B3LYP/6-31+G*. Energies are relative to separated reactants in kcal/mol.

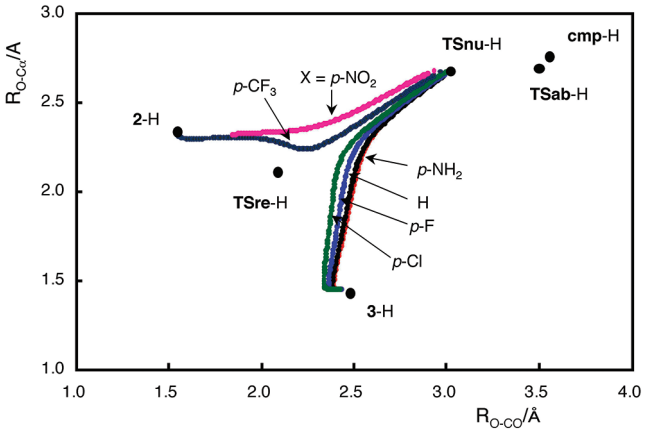

Figure 4. Two-dimensional map of IRC at B3LYP/6-31+G*. Black points represent stationary points for the parent compound, lines are IRC traces for substituted compounds from respective **TSnu**-X.

the substitution region ($R_{O-C\alpha}$ < 1.5 Å), whereas they were classified as addition when a trajectory reached the addition region (R_{O-CO} < 1.5 Å). It is clear that for the *p*-Cl-substituted derivative trajectories led to both product regions despite the fact that IRC gave the substitution product.

Table 3 summarizes the results of trajectory calculations for seven substituted derivatives. Figures under **2** and **3** are the number of trajectories that led to the addition and substitution product regions, respectively. Figures under **cmp** are the number of trajectories that gave back **cmp**, and those under **4** are the trajectories that gave **4** mainly through **cmp**. It is seen in Table 3 that in most cases trajectories gave all four products by going forward to **2** and **3** or going backward to **cmp** and further to **4**. More productive trajectories toward **2** and **3** were obtained with G03 than with PEACH, which is probably due to the difference in the initial sampling methods. Nevertheless, both methods gave the same tendency that % addition increases with the electron-withdrawing ability of substituent, in line with the tendency observed in the IRC calculations. These trajectory results indicate that a single TS gives two products through path bifurcation after the rate-determining TS, the ratio of the two products depending on the electronic nature of the substituent, or in other words, depending on the relative stability of **2** and **3** (Table 2). The situation is similar to previous reactions.[20−22] The present results add a new example of bifurcation in yet another type of basic organic reactions, namely, addition/substitution. It should be noted, however, that the present simulations were carried out for isolated gas-phase species, as in the previous studies, and hence the results do not ensure the occurrence of bifurcation in actual solution-phase organic reactions. It is thus hoped that a possible occurrence of path bifurcation for the reaction in solution would be examined by experiment as reported for the Beckmann rearrangement/fragmentation reactions.[26]

Effect of Internal Energy on Product Selectivity. The MD simulations of the parent compound at B3LYP/6-31+G* on G03 were carried out at four different initial kinetic energies: 2.8, 19.8, 36.8, and 53.8 kcal/mol. The results summarized in Table 4 show that the selectivity between **2** and **3** did not depend on the initial energy, but with higher initial energies there appeared trajectories that initially gave **2** and then further proceeded to give **3** via **TSre** (OH^- migration) or to give the epoxide intermediate (**5**) through **TSep**. It is interesting to note that 3 trajectories each

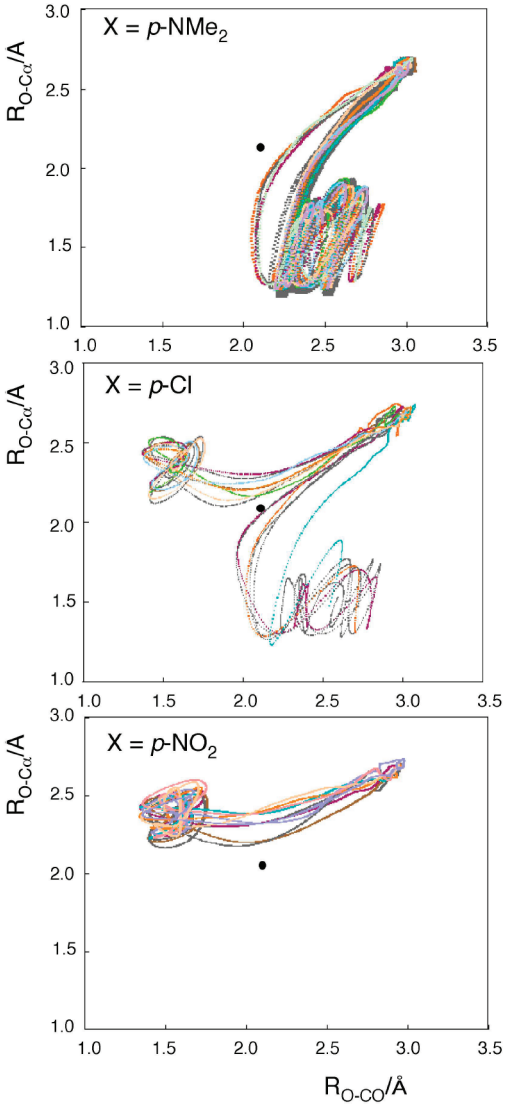

Figure 5. Two dimensional presentation of MD trajectories. Black points are the positions of **TSre**-X.

Table 3. Summary of MD Trajectories at B3LYP/6-31+G*[a]

X	N^b	cmp	4	2	3	% addition[c]
p-NMe_2	20 (20)	6 (4)	0 (0)	1 (0)	13 (16)	7 (0)
H	100 (100)	8 (43)	11 (2)	25 (7)	56 (48)	31 (13)
p-Cl	30 (30)	3 (16)	2 (0)	11 (8)	14 (6)	44 (57)
m-Cl	40 (30)	4 (13)	4 (3)	10 (9)	22 (5)	31 (64)
p-CF_3	40 (30)	3 (10)	2 (7)	19 (13)	16 (0)	54 (100)
p-CN	50 (30)	3 (11)	3 (5)	26 (12)	18 (2)	59 (86)
p-NO_2	30 (20)	0 (3)	3 (7)	23 (10)	4 (0)	85 (100)

[a] Number of trajectories calculated with G03. Numbers in parentheses are the results with PEACH. [b] Number of runs. [c] Percentage of addition trajectory given by **2**/(**2** + **3**).

with 19.8 and 36.8 kcal/mol and 4 with 53.8 kcal/mol gave **3** through **TSre**, whereas only 2 with 53.8 kcal/mol gave epoxide through **TSep**, despite the fact that **TSre** ($\Delta H^{\ddagger}$ = −37.7 kcal/mol) is less stable than **TSep** ($\Delta H^{\ddagger}$ = −40.7 kcal/mol). This is likely because in the initially formed **2** the C−OH stretching mode is

dx.doi.org/10.1021/jo201485y |*J. Org. Chem.* 2011, 76, 8294–8299

Table 4. Effect of Initial Kinetic Energy on the Fate of Trajectories from TSnu-H

initial energy[a]	N[b]	cmp[c]	2[d]	3
2.8	100	19 (11)	25 (0)	56
19.8	100	5 (3)	35 (3)	60
36.8	100	6 (3)	29 (3)	65
53.8	100	6 (4)	32 (6)	62

[a] Initial kinetic energy in kcal/mol. [b] Number of trajectories. [c] Number of trajectories that led to the **cmp** region. Numbers in parentheses are those that further afforded **4**. [d] Number of trajectories that led to **2**. Numbers in parentheses are those that further afforded **3** or epoxide.

excited, which may lead to OH^- migration prior to internal energy redistribution. Table 4 shows that the ratio of the backward trajectory (**cmp**) over the forward ones (**2** + **3**) is small with 2.8 kcal/mol initial kinetic energy and becomes even smaller for trajectories with higher initial energies. The reason for this is not clear, but it probably arose from the shape of the PES at the TS, which is favorable for forward trajectories when larger coordinate variations are allowed with higher kinetic energies in the initial sampling.

CONCLUSION

The reaction of α-haloketones with nucleophiles proceeds through a TS, where the n-orbital of a nucleophile interacts with the $\pi_{C=O}^*$ and $\sigma_{C-halogen}^*$ orbitals of the haloketones. Thus, the reactions of selected substrates and nucleophiles belong to borderline reactions, in which the mechanism varies from addition to substitution with the change of substrate structures. The present calculations for the reaction of $XC_6H_4COCH_2Br$ with OH^- revealed that there exists a single TS for the addition/substitution route and that the TS serves as the TS for direct substitution or as the TS for carbonyl addition depending on the electronic nature of the substituent. Trajectory calculations starting at a respective TS indicated that the single TS can serve for the two mechanisms, substitution and addition, through path bifurcation after the TS for borderline substrates. Thus, it has become now apparent that dynamic path bifurcation is a rather common phenomenon for fundamental reaction types of rearrangement,[20,21] elimination,[22] addition, and substitution reactions.

COMPUTATIONAL METHODS

Electronic structure calculations were carried out with the Gaussian 03 program suite.[24] Geometries were fully optimized at the B3LYP/6-31+G* level of theory. Vibrational normal-mode analyses were performed to ensure that each optimized structure was a true minimum or a saddle point on the PES. Unscaled frequencies were used to obtain thermochemical quantities, the thermal enthalpies, and free energies. Thermodynamic data used for enthalpy and free energy was computed at 298 K. Trajectory calculations were performed at B3LYP/6-31+G* starting at the TS of each substituted substrate with the BOMD keyword, which adopts the Hessian-based predictor-corrector method and quasiclassical normal-mode sampling. The Hessians were computed analytically using electronic structure calculations and updated for five steps. Trajectories were integrated with a step size of 0.25 amu$^{1/2}$ bohr with preset initial kinetic energy. The total energy was conserved to better than 10^{-5} hartree. Trajectory calculations were also carried out with PEACH,[20,25] in which trajectories were started at optimized transition structures.

ASSOCIATED CONTENT

Supporting Information. Calculated energies and geometrical coordinates of the species discussed in this paper. This material is available free of charge via the Internet at http://pubs.acs.org.

AUTHOR INFORMATION

Corresponding Author

*E-mail: substituent-effect@hiroshima-u.ac.jp; yamataka@rikkyo.ac.jp.

Present Addresses

[†]Department of Chemistry, Graduate School of Science, Hiroshima University, 1-3-1 Kagamiyama, Higashi-Hiroshima, Hiroshima 739-8526, Japan.

ACKNOWLEDGMENT

The study was in part supported by the SFR aid by Rikkyo University and a Grant-in-Aid for Scientific Research from the Ministry of Education, Science, Sports, Culture and Technology, Japan. The computations were partly carried out by using the computer facilities at the Research Institute for Information Technology, Kyushu University.

REFERENCES

(1) Bordwell, F. G.; Brannen, W. T., Jr. *J. Am. Chem. Soc.* **1964**, *86*, 4645. Halvorsen, A.; Songstad, J. *J. Chem. Soc., Chem. Commun.* **1978**, 327.
(2) Peason, R. G.; Langer, S. H.; Williams, F. V.; Mcguire, W. J. *J. Am. Chem. Soc.* **1952**, *74*, 5130.
(3) Shaik, S. S. *J. Am. Chem. Soc.* **1983**, *105*, 4359.
(4) Yousaf, T. I.; Lewis, E. S. *J. Am. Chem. Soc.* **1987**, *109*, 6137. Forster, W.; Laird, R. M. *J. Chem. Soc., Perkin Trans. 2* **1982**, 135. Kalendra, D. M.; Sickles, B. R. *J. Org. Chem.* **2003**, *68*, 1594.
(5) McLennan, D. J.; Pross, A. *J. Chem. Soc., Perkin Trans. 2* **1984**, 981.
(6) Hughes, E. D. *Trans. Faraday Soc.* **1941**, *37*, 603.
(7) Koh, H. J.; Han, K. L.; Lee, H. W.; Lee, I. *J. Org. Chem.* **2000**, *65*, 4706.
(8) Lutz, R. P. *J. Am. Chem. Soc.* **1968**, *90*, 3788.
(9) Ross, S. D.; Finkelstein, M.; Petersen, R. C. *J. Am. Chem. Soc.* **1968**, *90*, 6411.
(10) Yates, P.; Farnum, D. G.; Stout, G. H. *J. Am. Chem. Soc.* **1958**, *80*, 196.
(11) Thorpe, J. W.; Warkentin, W. *Can. J. Chem.* **1973**, *51*, 927.
(12) Kevill, D. N.; Kim, C.-B. *J. Org. Chem.* **2005**, *70*, 1490.
(13) Pasto, D. J.; Garves, K.; Serve, M. P. *J. Org. Chem.* **1967**, *32*, 774.
(14) Hummelen, J. C.; Wynberg, H. *Tetrahedron Lett.* **1978**, *19*, 1089.
(15) Stevens, C. L.; Weiner, M. L.; Freeman, R. C. *J. Am. Chem. Soc.* **1953**, *75*, 3977. Stevens, C. L.; Malik, W.; Pratt, R. *J. Am. Chem. Soc.* **1950**, *72*, 4758.
(16) Fabian, A.; Ruff, F.; Farkas, O. *J. Phys. Org. Chem.* **2008**, *21*, 988.
(17) Carpenter, B. K. *Acc. Chem. Res.* **1992**, *25*, 520. Carpenter, B. K. *Angew. Chem., Int. Ed.* **1998**, *37*, 3340. Carpenter, B. K. *J. Phys. Org. Chem.* **2003**, *16*, 858. Ess, D. H.; Wheeler, S. E.; Iafe, R. G.; Xu, L.; Çelebi-Ölçüm, N.; Houk, K. N. *Angew. Chem., Int. Ed.* **2008**, *47*, 7592. Yamataka, H. In *Advances in Physical Organic Chemistry*; Richard, J. P., Ed.; Academic Press: New York, 2010; Vol. 44, Chapter 10, p 173.
(18) Singleton, D. A.; Hang, C.; Szymanski, M. J.; Greenwald, E. *J. Am. Chem. Soc.* **2003**, *125*, 1176. Doubleday, C.; Suhrada, C. P.; Houk, K. N. *J. Am. Chem. Soc.* **2006**, *128*, 90. Ammal, S. C.; Yamataka, H. *Eur. J. Org. Chem.* **2006**, 4327. Leach, A. G.; Houk, K. N.; Foote, C. S. *J. Org. Chem.* **2008**, *73*, 8511. Kelly, K. K.; Hirschi, J. S.; Singleton, D. A. *J. Am. Chem. Soc.* **2009**, *131*, 8382.

(19) Taft, R. W. In *Progress in Physical Organic Chemistry*; Taft, R. W., Ed.; Wiley, New York, 1983; Vol. 14, Chapter 6, p 247.
(20) Yamataka, H.; Sato, M.; Hasegawa, H.; Ammal, S. C. *Faraday Discuss.* **2010**, *145*, 327.
(21) Katori, T.; Itoh, S.; Sato, M.; Yamataka, H. *J. Am. Chem. Soc.* **2010**, *132*, 3413.
(22) Itoh, S.; Yamataka, H. *Chem.—Eur. J.* **2011**, *17*, 1230.
(23) Yamataka, H.; Aida, M.; Dupuis, M. *Chem. Phys. Lett.* **1999**, *300*, 583. Bakken, V.; Danovich, D.; Shaik, S.; Schlegel, H. B. *J. Am. Chem. Soc.* **2001**, *123*, 130. Taketsugu, T.; Kumeda, Y. *J. Chem. Phys.* **2001**, *114*, 6973. Yamataka, H.; Aida, M.; Dupuis, M. *J. Phys. Org. Chem.* **2003**, *16*, 475. Li, J.; Li, X.; Shaik, S.; Schlegel, H. B. *J. Phys. Chem. A* **2004**, *108*, 8526. Ussing, B. R.; Hang, C.; Singleton, D. A. *J. Am. Chem. Soc.* **2006**, *128*, 7594. Çelebi-Ölçüm, N.; Ess, D. H.; Aviyente, V.; Houk, K. N. *J. Org. Chem.* **2008**, *73*, 7472.
(24) Frisch, M. J. et al. *Gaussian 03, Revision E.01*; Gaussian, Inc.: Wallingford, CT, 2004.
(25) Komeiji, Y.; Uebayasi, M.; Takata, R.; Shimizu, A.; Itsukashi, K.; Taiji, M. *J. Comput. Chem.* **1997**, *18*, 1546. Komeiji, Y.; Ishikawa, T.; Mochizuki, Y.; Yamataka, H.; Nakano, T. *J. Comput. Chem.* **2009**, *30*, 40.
(26) Yamamoto, Y.; Hasegawa, H.; Yamataka, H. *J. Org. Chem.* **2011**, *76*, 4652.